3074
doi:10.1017/S1431927621010643

Microsc. Microanal. 27 (Suppl 1), 2021

Structural Alloys in Light Water Reactor Systems: Role of Microscopy in the Mitigation of Environmentally-Assisted Cracking Through Surface Optimisation

M.G. Burke

University of Manchester, Manchester, United Kingdom

Environmentally-assisted cracking (EAC) includes materials degradation phenomena such as primary water stress corrosion cracking (PWSCC) and corrosion fatigues in pressurised water reactor (PWR) systems. Extensive research has ben performed to evaluate and assess material susceptibility to these phenomena as well as to the specific environmental conditions that may promote such degradation. As EAC (including PWSCC) is generally assumed to consist of 2 parts - initiation and propagation, it is the initiation stage that can take several years or several decades, followed by more rapid crack propagation. The Horizon 2020 project MEACTOS - Mitigating EAC Through the Optimisation of Surface Condition - is a multi-national European research project focused on the effect of various surface treatments on the EAC initiation in light water reactor environments. In MEACTOS, a Ni-base Alloy 182(A182) overlay deposits was subjected to various surface treatments, including advanced machining techniques, prior to slow strain rate tensile (SSRT) tests in relevant environments. Fundamental to this project is a thorough understanding of the effect of surface treatments on the near-surface microstructure of the materials. In this study, the effect of standard industrial machining (STI) and surface advanced machining (SAM) on local surface/near-surface microstructural evolution is examined.

The as-machined Alloy 182 overlay specimens were characterised using a Zeiss Merlin FEG-SEM equipped with an Oxford Instruments X-MAX 150 and X-Max Extreme SDDs, an EBSD detector and Aztec analysis system, an FEI Tecnai T20 S/TEM and an FEI Helios 660 FIB/SEM. Metallographically-prepared cross-section specimens were evaluated to examine the extent of machining-induced microstructural changes in the near-surface regions that would be in contact with the primary water environment. BSE imaging permitted the assessment of the machining-induced deformation via channelling contrast associated with the heavily dislocated A182. Examples of the local microstructures for the two surface machining treatments are presented in Figure 1, which revealed very complex microstructures within approximately 30 μm of the as-machined surfaces. These near-surface modified microstructures consisted of an ultra fine-grained (UFG) layer that varied in extent from ~2 to 6 μm from the surface for the STI condition. Beneath this layer was a heavily deformed zone that extended another ~20-25 μm. In contrast the SAM treatment resulted in a more consistent UFG layer that extended ~ 2-3 μm. The BSE image (Figure 1b) revealed extensive deformation as manifested by a high proportion of slip bands with ~ 30 μm below the UFG layer.

FIB lift-out cross-section TEM specimens were prepared and analysed for further characterize the nature of the UFG layer for both the STI and SAM treatments. TEM analysis, electron diffraction and transmission Kikuchi diffraction (TKD) were used to determine the size of the nanoscale grains in the UFG layers. TEM characterization revealed that the UFG consisted of randomly orientated grains that ranged in size from ~15 to 200 nm, and that these grains exhibited evidence of deformation. The deformed layer beneath the UFG was charcterized by extensive deformation of the coarse A182 dendritic grains from the STEM machined specimens whereas a deformed elongated/ "pancaked" grain structure was observed beneath the UFG in the SAM specimens. These pancaked grains were ~100 to 500 nm in length and ~ 20 to 100 nm in thickness. The nature of these modified microstructures affects the oxidation response of these materials. In particular, the presence of an UFG layer has been demonstrated for as-machined Type 316L stainless steels, thereby reducing the cracking response under SSRT conditions. However, the additional cold-work resulting from the machining operations affects local hardening, which can also affect the initiation and propagation of cracks. Therefore, optimised machining treatments that minimise the deformed zones can provide a benefit in terms of the local precursor stages in the initiation of EAC behavior in light water reactor systems. In particular, detailed microstructural analysis is critical to identify and assess these pronounced near-surface microstructural changes in LWR structural alloys.

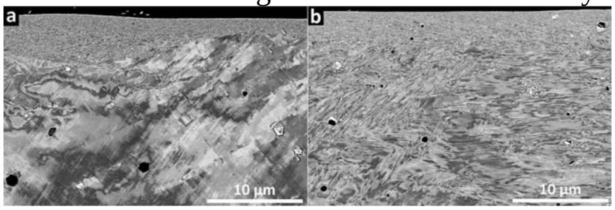

Figure 1. Figure 1: BSE images of cross-section specimens from the (a) STI, and (b) SAM treatments. Note the presence of the UFG layer adjacent to the surface, with significant subsurface machining-induced deformation in these A182 samples.

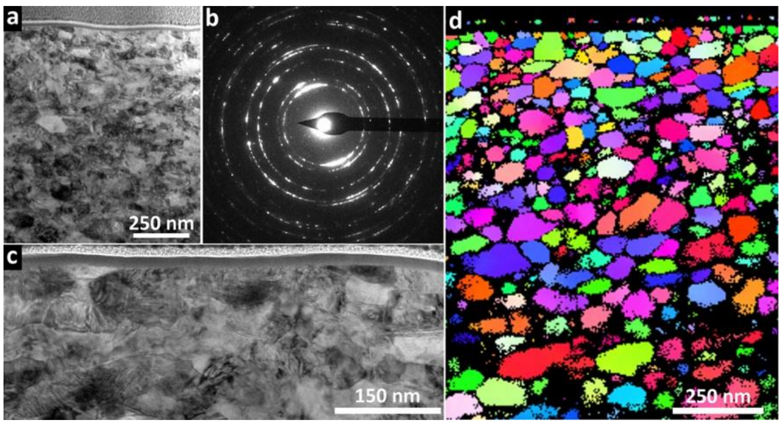

Figure 2. Figure 2: Characterisation of the near-surface region of FIB lift-out specimen from the STI machined sample: (a) BF TEM image of UFG layer; (b) SADP of the randomly oriented UFGs; (c) BF TEM image of the UFGs and a thin ~15 nm carbonaceous surface layer associated with lubricant; (d) TKD IPF of the UFG layer.

References

[1] L. Chang et al., **Corrosion Sci., 138** (2018) 54-65.

[2] This project received funding from the Euratom research and training programme 2014-2018 under grant agreement 755151.

https://doi.org/10.1017/S1431927621010643 Published online by Cambridge University Press